Cool Customers in the Stellar Graveyard III: Limits to Substellar Objects around nearby White Dwarfs using CFHT

John H. Debes[1,2], Jian Ge[3],Christ Ftaclas[4]

ABSTRACT

Results from a groundbased high contrast imaging survey of thirteen nearby white dwarfs for substellar objects is presented. We place strict upper limits on the type of substellar objects present, ruling out the presence of anything larger than ∼14 M_{Jup} for eight of the white dwarfs at separations >19 AU and corresponding to primordial separations of ∼3-6 AU assuming adiabatic mass loss without tidal interactions. With these results we place the first upper limit on the number of intermediate mass stars with brown dwarfs at separations > 13 AU. We combine these results with previous work to place upper limits on the number of massive Jovian (> 10 M_{Jup}) planets in orbit around white dwarfs whose progenitors spanned a mass range of 1-7 $M_{\odot}$.

Subject headings: circumstellar matter–planetary systems–white dwarfs

1. Introduction

White dwarfs (WDs), the end state of stellar evolution for ∼1-8 $M_{\odot}$, are a population of stars that potentially hold an important key to directly imaging extrasolar planets (Burleigh et al. 2002). They present several advantages compared to main sequence stars for strategies that rely on high contrast imaging. Due to their dense nature, WDs have small radii and cooling atmospheres that translate to surface fluxes orders of magnitude dimmer than their main sequence progenitors. Since they are hotter than any putative substellar companion, the companion's flux peaks well into the Rayleigh-Jeans tail of the WDs emission. These

[1]Department of Astronomy & Astrophysics, Pennsylvania State University, University Park, PA 16802

[3]Department of Astronomy, University of Florida, Gainesville, Fl 32611

[4]Institute for Astronomy, University of Hawaii, Honolulu, HI 96822

[2]Based on observations obtained at the Canada-France-Hawaii Telescope (CFHT) which is operated by the National Research Council of Canada, the Institut National des Science de l'Univers of the Centre National de la Recherche Scientifique of France, and the University of Hawaii.

two factors allow a modest contrast difference between the white dwarf and any possible substellar companions.

This is the third paper in a series that take slightly different approaches in the search to directly image a nearby extrasolar planet and place limits on what type of companions could be present around each WD. The first, Debes et al. (2005a, hereafter DSW05a), looked specifically at the WD G 29-38 but utilized 2MASS photometry, pulsational timing, Gemini North Telescope high contrast imaging, and Hubble Space Telescope (HST) coronagraphic images to constrain the presence of planets and brown dwarfs at distances from 0.1 AU to 50 AU. The second paper, Debes et al. (2005b, hereafter DSW05b), relied on 2MASS data and HST data to once again constrain the presence of planets and brown dwarfs around DAZ WDs, WDs with hydrogen atmospheres and the presence of weak metal line absorption. We extend that search now to nearby white dwarfs with well modeled ages and measured parallaxes from the ground. For a majority of our targets we used the sample of Bergeron et al. (2001).

We search for planets and brown dwarfs with imaging using the PUEO/KIR instruments on the Canada France Hawaii Telescope (CFHT). This initial survey is intended to demonstrate that useful detections of substellar and planetary objects are possible with a large enough sample of nearby white dwarfs from the ground.

In Section 2 we present the observations we performed and in Section 3 we discuss how our observations were analyzed. In Section 4 we present the candidate companions we have discovered as well as any background objects that may be present. Several of these companions can be ruled out through the use of second epoch observations. For one WD, WD 0208+396, we provide second epoch information for a candidate discovered in DSW05b. In Section 4 we determine the limits to companions that we could have detected. Finally in Section 5 we summarize our results and synthesize them with the results of previous work.

2. Observations

Observations of all the white dwarfs were taken during three trips to CFHT–the first on October 11-14 2003, the second on April 1, 2004, and the final on September 29, 2004. Observations were taken primarily in the J band on the first run and in the H band on the second and third run using the KIR instrument in conjunction with PUEO, the wavefront curvature AO system (Rigaut et al. 1998). Table 1 shows the list of targets including their V magnitudes, masses, primordial masses, estimated ages, effective temperatures, and distances. The mass, T_{eff}, and cooling age came from either Bergeron et al. (2001) or Liebert

et al. (2004), with the exception of WD 0501+527. WD 0501+527's parameters come from Finley et al. (1997). The primordial mass (M_i) was calculated by a theoretical initial to final mass function given by $M_i = 10.4 \ln[(M_{WD}/ M_\odot)/0.49] M_\odot$ (Wood 1992). The main sequence lifetime of the star was determined by $t_{MS} = 10 M_i^{-2.5}$ Gyr (Wood 1992). Since these relations only work well for $M_{WD} > 0.54 M_\odot$, WD 0501+527's total age is unknown.

The very advantage these targets have for detecting planets is offset by the fact that most current AO systems cannot reliably correct atmospheric turbulence for such faint objects. With most large telescope AO systems requiring targets with $V \lesssim 13$, most of these targets would have to be imaged without the help of AO. However, the curvature wavefront sensor AO system of PUEO provides a heightened advantage by being able to guide on targets with $V \lesssim 16$, allowing most nearby WDs to be accessible to AO correction (Rigaut et al. 1998). AO correction is particularly useful for gaining spatial resolution as well as sensitivity against the near-IR background, the wavelength at which cool substellar objects become observable with current telescopes. These two benefits allow the more modestly sized CFHT to compete realistically with larger telescopes in this area without AO, as well as with space based near-IR imaging.

Table 2 shows our list of observations as well as total integrations for each target WD. Most objects were observed for ∼1 hr using 240s sub-exposures that were dithered in a 5″ five point grid pattern for background subtraction. This left a ∼20″×20″ field of high sensitivity. WD 1213+568 and WD 1633+572 had shorter total exposure times, with 15 minutes and 16 minutes respectively. WD 0208+396, WD 0501+527, and WD 2341+321 had longer integrations of 90 minutes, 66 minutes, and 78 minutes, respectively. During these observations high levels of relative humidity forced the telescope to be shut down for short periods of time, which resulted in a repetition of some positions of our dither pattern on the sky. Objects that threatened to saturate the detector had shorter sub-exposures. This was the case for WD 1213+568 and WD 2140+207 whose sub-exposures were 60s and 120s respectively. Flatfields were taken at the beginning of each night.

As can be seen from Table 1, our targets ranged in brightness, which in turn affected the performance of the AO correction. Correction deteriorated towards dawn on our second run as the sky background increased, and weather conditions varied throughout our first run. The third run had spectacular seeing throughout most of the night (0.5″-0.6″ in V), allowing diffraction limited images to be taken of WD 2140+207, WD 2246+223, and WD 2341+321. Throughout much of the second run, when most of our targets were taken, the full width half maximum (FWHM) of our final images ranged from ∼140 milliarcseconds to ∼200 milliarcseconds, compared to a diffraction limited FWHM of 120 milliarcseconds. WD 0501+527's final FWHM was 132 milliarcseconds, compared to the J band diffraction

limited FWHM of 90 milliarcseconds.

3. Data Analysis

All data were flatfielded, background subtracted, registered, and combined into final images. These final images were used for two purposes: for deep background limited imaging far from the central target star and as point spread function (PSF) reference stars for other observations. Due to dithering, the highest sensitivity was generally within 7″ of the target star.

In order to gain contrast close to each target white dwarf, we also employed PSF subtraction to get high contrast to within 1″. To achieve good results, each registered sub-exposure was subtracted from another reference PSF image; preferably from a reference that was brighter than the target and that had a similar FWHM. The subtraction images were median combined to produce the final subtracted image. In the case of WD 1121+216 and WD 1953-011, there was a brighter star in the field and that was used as a simultaneous reference. Even though observations were separated by timescales on the order of hours, we were able to get subtraction that suppressed the PSF by 3-4 magnitudes at 0.8″(see Figure 1), with a higher sensitivity typically achieved in the non-subtracted images beyond 2″. PSF subtraction was not possible for WD 1213+528, WD 0208+396, and WD0521+527, since no suitable reference was available. Figure 1 shows a comparison before and after PSF subtraction with a contemporaneous reference for WD 1953-011.

Any point sources that were detected had their flux measured by adding the counts within an aperture comparable to the FWHM of the particular image and comparing the counts in the same size aperture with the target star. A differential H magnitude was computed and then added to the 2MASS H magnitude of the WD, taking into account the transformation from the 2MASS system to the MKO system. Since AO PSFs tend to vary with time photometric accuracy is limited by this variation and we found it preferable to use differential magnitudes since to zeroth order all PSFs in an image should be varying in the same manner. The large isoplanatic patch of PUEO makes this a reasonable assumption (Rigaut et al. 1998). Extended objects were interpreted to be background galaxies and had their total flux measured within a 0.5″ radius aperture and compared to the flux of the target star in the field. Typically, most of the light from a star was captured within a 1.5″ radius aperture, such that larger apertures changed the instrumental magnitude by ∼0.01 mag or less.

4. Candidate Companions and Background Objects

Many targets showed nothing besides the primary in the field of view. However, six of the targets had other objects in the field which we designated as potential candidates. Any candidate would have to be unresolved. Where second epoch images were available, we used them to determine if any candidate was co-moving with the primary. If any second epoch images showed no common proper motion that candidate was eliminated. Two candidates do not have second epoch information and remain as viable brown dwarf candidates. Several of the higher latitude targets also had nearby resolved galaxies within 10″, which we note in case they are useful for future groundbased study; such as with laser guided AO or multi-conjugate AO. Table 3 gives their positions and H band magnitudes within a 0.5″ aperture. One object, DSW 1, has already been presented in DSW05b, but here we add its MKO H magnitude from our CFHT observations.

4.1. WD 2341+321

WD 2341+321 has two candidate point sources–C1 and C2–that cannot be refuted with second epoch POSS images. Both are too faint to have been detected. C1 is at an R of 9.17″±0.01 and a PA of 116°±1, with an H magnitude of 18.5. C2 is detected closer in, after PSF subtraction. Figure 2 shows the original image and after PSF subtraction. This dimmer candidate is more promising since it is closer to the target WD, and is detected at a S/N of 7 with an H magnitude of 22.3. It has an R of 2.25″ and PA of 72.5°±1. If both are physically associated with WD 2341+321, they would be 27 M_{Jup} and 13 M_{Jup} respectively. At a distance of 16.6 pc, they would have orbital separations of 37 AU and 152 AU corresponding to primordial separations of 13 AU and 54 AU, given a current WD mass of 0.57 $M_\odot$ and an inferred initial mass of 1.6 $M_\odot$. However, they cannot be ruled associated until they demonstrate common proper motion with WD 2341+321. WD 2341+321's proper motion is 0.21″/yr, so it should be relatively easy to determine common proper motion within a year (Perryman et al. 1997).

4.2. WD 1121+216

WD 1121+216 has a brighter star ∼5″ away. Inspection of POSS plates clearly shows that it is a relatively fixed background star and it is not a common proper motion companion. After PSF subtraction, WD 1121+216 shows emission that at first glance appears to be a dust disk or blob ∼ 20 AU from the WD. Figure 3 shows the emission. It is clearly visible

both in the original image and after PSF subtraction. Inspection of the POSS 2 B plate shows that it is most likely a background galaxy, as there is an extended source at the position of the emission currently seen near the WD. Caution should be taken with high latitude objects that appear to show extended emission as a background galaxy can be mistaken for circumstellar emission. Any such discovery should show common proper motion to be credible. The background galaxy has a surface brightness of 20.1 mag/$\Box''$. This detection demonstrates that we could have discovered any circumstellar emission for our targets at approximately this level.

4.3. WD 1213+528

WD 1213+528 shows a candidate companion $\sim 8''$ to the south, but inspection of POSS 2 plates shows that this object is not a common proper motion companion.

4.4. WD 1953-011

WD 1953-011 has several nearby background sources, which are well separated. Most are visible on POSS plates and due to WD 1953-011's proper motion are easily discarded as possible proper motion companions. The brightest background object in the field, $\sim 7''$ to the South, has a noticeable companion at a separation $1.08'' \pm 0.01$, PA= $88.6^\circ \pm 0.3$ with a ΔH=7.6. Figure 4 shows the star before and after PSF subtraction and Gaussian smoothing.

A spectrophotometric SED using POSS B, V, R, and I magnitudes and 2MASS J,H, and Ks magnitudes of the background star makes it consistent with either a $\sim$M0 dwarf at $\sim$300 pc or a K2 giant at $\sim$10 kpc (Allen 1999). If it is a main sequence star, the companion would be a 0.07-0.08 $M_\odot$ object according to the models of Baraffe et al. (2003). If it is instead a giant, the companion is an M dwarf. The former explanation of a nearby M dwarf host star with a low mass companion seems more plausible given the low galactic latitude of the source and the apparent lack of significant reddening. It is also possible the two stars are not physically associated. Despite the fact that this is not relevant to our current study, this discovery demonstrates the efficacy of our PSF subtraction technique.

4.5. WD 2140+207

WD 2140+207 has a dim, point-like object $\sim 5''$ away, with several point sources and galaxies in the surrounding field. Most of the point sources can be discriminated as back-

ground objects from POSS plates, including the near object discovered. With the help of POSS PSF subtraction, a marginal detection of the companion was possible on the POSS 2 B plate. At epoch 1990.57, the time of the observations taken by POSS, the separation of the object had an R of 8.58″with a PA of 239.6° east of north. In our CFHT observations the object had an R of 5.88 and a PA of 296.7°. This is clearly a background object.

4.6. WD 0208+396

Two candidate objects as well as a galaxy ∼8″ away were discovered in HST images presented in DSW05b. The point source candidates were re-imaged on our third visit to CFHT ∼1 year later and their H magnitudes measured. Figure 5 shows the images at the two epochs. C1 and C2 had H magnitudes of 19.35 and 22.22 respectively. In order to determine whether any of the candidates had common proper motion we needed to compare their positions relative to the HST observations in DSW05a. In those observations the C1 was found to be at a separation of 8.60°±0.1 and a PA of 175°±1. Its F110W magnitude was 20.64±0.01. WD 0208+396 has a proper motion of 1069 mas/yr in RA and -523 mas/yr in Dec, which allows us to predict the position of the C1 if it is not co-moving. We predict C1's position with respect to WD 0208+396 to be ΔRA=-0.41″±0.1 and ΔDec=-8.03″±0.1. We find that the candidate is measured at a position ΔRA=0.03″ and ΔDec=-8.02″. C2 has an F110W magnitude of 23.5±0.1 and in the HST image had an R=10.33″±0.2 with a PA=169°±2. Its predicted position if not co-moving was predicted to be ΔRA=0.82″±0.1 and ΔDec=-9.60″. The measured relative position was ΔRA=1.27″ and ΔDec=-9.51″. There is a systematic, significant difference between the predicted ΔRA and that measured for both candidates which are also spatially close. Measurements of the relative position of the galaxy in the field also shows a similar discrepancy in where its relative position should be (it's obviously not co-moving) which supports the explanation that the CFHT field is rotated clockwise by ∼1.7°, which places all of the measured positions within the errors of the predicted positions. Therefore, we can state with certainty that the candidates are both background objects.

5. Limits to Companions

Since many targets did not have any possible companions, it is instructive to place limits on what kind of objects could be detected around each target. We can place limits both for resolved and unresolved companions by the combination of our imaging results and the measurement of these objects' measured flux in comparison with their expected flux.

5.1. Imaging

For our images, we followed the same strategy for determining our imaging sensitivity as in DSW05a and DSW05b. This strategy is to implant artificial companions into our images and try to recover them at a S/N of 5, in order to test the sensitivity of our observations. The main difference for AO imaging is that the PSF is not stable, so we use a version of our target WD PSF normalized to 1 DN. The implant would be scaled by a value, placed within the field and an aperture approximately equal to the implant's core FWHM was used to determine the S/N. If the S/N was >5, then the implant was considered recovered, otherwise the implant's scaled value was increased. Values at 20 different angular locations were determined at each radius, for azimuthal averaging. The median of the different values was taken to give a final azimuthal averaged sensitivity. Relative photometry with respect to the target WD (or another unsaturated object in the field) was calculated and the 2MASS H magnitude for the target WD was used to determine a final sensitivity. Figure 6 shows a typical sensitivity curve with PSF subtraction.

The values were then used with a grid of substellar spectral models to determine what kind of substellar object a limiting magnitude would correspond to at the particular distance and age of the WD system. Specifically, we used the models of Baraffe et al. (2003), primarily because they had isochrones that spanned the mass range and age of interest to our target WDs. The magnitudes were cross checked with the models of Burrows et al. (2003) and for isochrones that overlapped they provided similar results to within a magnitude or to within 1 or 2 M_{Jup}, thus giving us confidence that we could combine our results here with those in DSW05b. Using interpolation, we turned the observed sensitivities to specific masses at the particular ages of the WDs. Table 4 shows the final sensitivities for each WD.

5.2. Near-IR Photometry

While direct imaging is most sensitive to companions $>1''$ unresolved companions could still be present for some of these targets. In order to rule out companions at separations where imaging or PSF subtraction could not resolve them, we turn to the near-infrared fluxes of these objects provided by 2MASS photometry (Cutri et al. 2003). Using the measured effective temperatures, gravities, and distances of the WDs given in the literature, we can model the expected J, H, and Ks fluxes based on the models of Bergeron et al. (1995). If the photometry is of a high enough accuracy, one can place limits on the type of excesses present for these objects. These limits allow us to understand what types of companions and dusty disks are ruled out. The details of this process have already been described in DSW05a. For our targets, the majority come from Bergeron et al. (2001), but the WD 2341+321

parameters came from Liebert et al. (2004). DSW05b calculated the estimated 1 σ limits for both samples in the J, H, and K_s filters to be 0.04, 0.04, and 0.05 mag respectively for the Bergeron et al. (2001) sample. For the sample of Liebert et al. (2004) we found that the limits are 0.07, 0.10, and 0.15 for J, H, and K_s respectively.

The one exception is WD 0501+527, whose parameters are taken from Finley et al. (1997). The distance to WD 0501+527 is determined from its Hipparcos parallax (Perryman et al. 1997). In the Finley et al. (1997) sample, only spectroscopic properties were determined, so no attempt to model the distance was made. Due to a lack of modeled distance, we cannot estimate the rough error in the modeling as an ensemble. Rather, we compare ΔJ to the quoted photometric errors in 2MASS. The errors in J are $\sim$0.02, and since ΔJ falls within this range, we use this as our estimate for a significant excess, which we determine to be an excess of 0.06 in J. Since WD 0501+527 is so hot, its cooling time is $\ll$1 Gyr and its total age depends entirely on its initial mass. Unfortunately this is unknown, so we calculate possible companion limits given a range of possible main sequence ages for this WD.

All of our other objects show no significant excess as well so we need to determine to what mass limit we could have detected an excess in our sample. Taking the substellar models of Baraffe et al. (2003), we took the 3σ limits and interpolated between the models to fit the estimated total ages of the white dwarf targets. We find that for all of our targets, any object more massive than $\sim$69 M_{Jup} would have been detectable in the 2MASS search. Therefore, all targets should not have any stellar companions present at close separations. The exceptions to the limit are WD 1213+568, which already has an unresolved companion M dwarf, and WD 0501+527, which is less sensitive due to its large T_{eff}. Any further excess beyond the companion of WD 1213+568 cannot be determined. Table 4 shows our results for unresolved and resolved companion sensitivities. For the excess limits we take into account the distance to the WD to obtain a limit on the absolute magnitude of an object that could create an excess.

6. Discussion

We have surveyed thirteen white dwarfs for substellar objects. From this search we have found two potential candidates both around the white dwarf WD 2341+321. This star requires follow-up observations to confirm or refute these candidates. If any of the companions is confirmed to be co-moving, they are dim enough to be consistent with substellar mass objects. To date, only two substellar objects are known to be in orbit around nearby WDs (Zuckerman & Becklin 1992; Farihi & Christopher 2004). With putative absolute magni-

tudes in the H band of ∼21-22, these would be hard to confuse with higher mass objects such as in young stellar populations (Mohanty et al. 2004).

To date, nine hydrogen white dwarfs with metal lines, so-called DAZs, have been searched for substellar objects–seven from our observations with HST and two from the ground. WD 1633+433 and WD 1213+529 both have been found to have small amounts of metals such as Ca in their atmospheres (Zuckerman et al. 2003). WD 1213+529 has an unresolved stellar companion, while WD 1633+433 appears from its 2MASS photometry and our imaging to be devoid of anything > 14 $M_{Jup} > 15$ AU away and > 48 M_{Jup} at separations < 15 AU. Given that ∼25% of DAs have measurable metal lines and their explanation seems less likely due to ISM accretion and more due to unseen companions, either substellar or planetary, they are interesting targets for faint companion searches (Zuckerman et al. 2003; Debes & Sigurdsson 2002).

Using a binomial type distribution that has been used to calculate the frequency of brown dwarf companions to nearby stars, we can calculate limits to the frequency of substellar objects around DAZs as well as our full sample of 20 white dwarfs (McCarthy & Zuckerman 2004). That distribution is given by

$$P(f,d) = f^d(1-f)^{N-d}\frac{N!}{(N-d)!d!} \quad (1)$$

where P is the probability, f the true frequency of objects, N the number of observations, and d the number of successful detections.

If one integrates over all the probabilities, one can derive limits that encompass 68% of the distribution. From these limits we can compare our results with both the radial velocity surveys and imaging surveys for brown dwarfs. In this study we can place meaningful limits to planet and brown dwarf formation around stars that originally had masses between $1.5M_{\odot}$-$7M_{\odot}$, the range of initial masses inferred for our targets. From our limit of $\sim 1''$ as the innermost separation where we could have detected a companion for all of our targets, we can derive an innermost projected orbital separation that we probed. Since any companion that is found today in an orbit with semi-major axis a had a primordial orbit M_f/M_i times smaller before the star lost its mass and turned into a white dwarf, we can probe inwards to regions that should have been sites for planet formation. With a subset of our targets sensitive to planetary mass objects at separations that would be where planets with orbits like Jupiter would be found we can study a region of parameter space complementary to radial velocity surveys (Marcy & Butler 2000). Since our observations are also sensitive to brown dwarfs we also complement surveys for widely separated brown dwarf companions to white dwarfs (Farihi et al. 2005).

For our samples we neglect WD 0501+527 and WD 1213+529, since the observations

of these targets are significantly less sensitive than the other observations. Of the 18 remaining WDs from the DSW05b and CFHT samples, eight are DAZs and the rest are a mixture of other white dwarf spectral types including DAs with no detectable metals in their atmospheres.

In our DAZ sample, which includes those objects observed in DSW05b, WD 1633+433 and WD 1213+528, the images of four WDs were sensitive enough to detect planets and none were found. Therefore, they do not have planetary mass objects > 10 M_{Jup} at projected separations > 21 AU, corresponding to an inferred minimum primordial separation of > 6 AU. When we integrate over all possible probabilities we get an inferred limit of <20% for the frequency of massive planets in orbit around DAZs. Assuming that every DAZ may possess a planetary system, this is within a factor of 4 to the frequency of massive planets discovered with the radial velocity surveys with $M\sin(i) > 10M_{Jup}$, where 6 of 118 discovered planetary systems[1] possess such companions <5-6 AU as well as radial velocity surveys of G giants (Marcy & Butler 2000; Sato et al. 2003). Furthermore, none of the eight apparently single DAZs showed the presence of companions >70 M_{Jup} in close, unresolved orbits. This implies that <12% of DAZs have companions that are stellar. Any unseen object that could pollute a WD would have to be substellar for the majority of current apparently single DAZs.

For our total sample of 18 WDs, we can also place limits on any object > 19 M_{Jup} present at projected separations > 34 AU and corresponding to a minimum primordial orbit of > 10 AU. From zero detections in this sample, we infer that intermediate mass stars from between 1.5-7$M_{\odot}$ have brown dwarf companions <6% of the time. Also, for our entire sample of nearby white dwarfs, seven of the eighteen were sensitive enough to detect massive planets (M> 10 M_{Jup}) at projected separations of > 21 AU, with inferred primordial separations of >6 AU. Therefore, the upper limit for the presence of massive planets around intermediate mass stars is <13%. If we also include the results of a planet search amongst single white dwarfs in the Hyades, we can effectively double our sample size of targets sensitive to massive planets (Friedrich et al. 2005). In the Friedrich et al. (2005) survey, they found no planets > 10 M_{Jup} at separations >23 AU, corresponding to primordial separations of ∼5 AU. Combined with our results, the upper limit for massive planets around single white dwarfs (at 68% confidence) is then closer to 7%.

High spatial resolution imaging of white dwarfs will also be important as supporting observations for Spitzer observations of white dwarfs that are looking for mid-IR excesses due to substellar companions. WD 1121-216 in particular may falsely show an excess due to it temporarily being coincident with a background galaxy. Approximately 100 WDs have

[1]http://www.obspm.fr/encycl/encycl.html

been approved to be observed with Spitzer in the Cycle 1 GO programs. A combination of the Spitzer photometry and imaging would provide a more sensitive test for unresolved companions while providing a check against source confusion due to Spitzer's larger PSF with the IRAC camera, for example (Fazio et al. 2004). A large survey like that would also start placing rigorous limits on the presence of faint companions to nearby white dwarfs.

JD and JG acknowledge partial support by NASA with grants NAG5-12115, NAG5-11427, NSF with grants AST-0138235, and AST-0243090. CF acknowledges support from NSF with grant AST-9987356.

REFERENCES

Allen, D. 1999, Allen's Astrophysical Quantities

Baraffe, I., Chabrier, G., Barman, T. S., Allard, F., & Hauschildt, P. H. 2003, A&A, 402, 701

Bergeron, P., Leggett, S. K., & Ruiz, M. T. 2001, ApJS, 133, 413

Bergeron, P., Wesemael, F., Lamontagne, R., Fontaine, G., Saffer, R. A., & Allard, N. F. 1995, ApJ, 449, 258

Bleach, J. N., Wood, J. H., Catalán, M. S., Welsh, W. F., Robinson, E. L., & Skidmore, W. 2000, MNRAS, 312, 70

Burleigh, M. R., Clarke, F. J., & Hodgkin, S. T. 2002, MNRAS, 331, L41

Burrows, A., Sudarsky, D., & Lunine, J. I. 2003, ApJ, 596, 587

Cutri, R. M., et al. 2003, VizieR Online Data Catalog, 2246, 0

Debes, J. H. & Sigurdsson, S. 2002, ApJ, 572, 556

Debes, J. H., Sigurdsson, S., & Woodgate, B. 2005a, (ApJ, in press)

—. 2005b, AJ, in press

Farihi, J., Becklin, E. E., & Zuckerman, B. 2005, ArXiv Astrophysics e-prints

Farihi, J. & Christopher, M. 2004, AJ, 128, 1868

Fazio, G. G., et al. 2004, ApJS, 154, 10

Finley, D. S., Koester, D., & Basri, G. 1997, ApJ, 488, 375

Friedrich, S., Zinnecker, H., Brandner, W., Correia, S., & McCaughrean, M. 2005, in ASP Conf. Ser. 334: 14th European Workshop on White Dwarfs, 431–+

Liebert, J., Bergeron, P., & Holberg, J. B. 2004, ArXiv Astrophysics e-prints

Marcy, G. W. & Butler, R. P. 2000, PASP, 112, 137

McCarthy, C. & Zuckerman, B. 2004, AJ, 127, 2871

Mohanty, S., Jayawardhana, R., & Basri, G. 2004, ApJ, 609, 885

Perryman, M. A. C., et al. 1997, A&A, 323, L49

Rigaut, F., et al. 1998, PASP, 110, 152

Sato, B., et al. 2003, ApJ, 597, L157

Wood, M. A. 1992, ApJ, 386, 539

Zuckerman, B. & Becklin, E. E. 1992, ApJ, 386, 260

Zuckerman, B., Koester, D., Reid, I. N., & Hünsch, M. 2003, ApJ, 596, 477

Table 1. List of WD Targets

WD	V	M_f ($M_\odot$)	M_i ($M_\odot$)	T_{eff} (K)	D (pc)	Total Age (Gyr)	References
0208+396	14.5	0.60	2.1	7310	16.7	2.9	1
0501+527	11.8	0.53		61000	68.8		2
0912+536	13.8	0.75	4.4	7160	10.3	2.8	1
1055-072	14.3	0.85	5.7	7420	12.2	3.0	1
1121+216	14.2	0.72	4.0	7490	13.4	2.2	1
1213+528	13.3	0.64	2.8	13000	38.6	1.0	3,4
1334+039	14.6	0.55	1.2	5030	8.2	10.2	1
1626+368	13.8	0.60	2.1	8640	15.9	2.6	1
1633+433	14.8	0.68	3.4	6650	15.1	2.8	1
1633+572	15.0	0.63	2.6	6180	14.4	3.8	1
1953-011	13.7	0.74	4.3	7920	11.4	1.9	1
2140+207	13.2	0.62	2.4	8860	12.5	2.1	1
2246+223	14.4	0.97	7.1	10330	19.0	1.7	1
2341+321	12.9	0.57	1.6	12570	16.6	3.4	3

References. — (1) Bergeron et al. (2001) (2) Finley et al. (1997) (3) Zuckerman et al. (2003) (4) Bleach et al. (2000)

Table 2. Observations

WD	Date(UTC)	Filters	Total Integration(s)
0208+396	11:10:46 2004-09-30	H	5280
0501+527	14:22:43 2003-10-11	J	3840
	15:12:45 2003-10-12	K	1920
0912+536	06:33:58 2004-04-02	H	3600
1055-072	08:12:16 2004-04-02	H	3600
1121+216	09:24:38 2004-04-02	H	3600
1213+528	10:47:20 2004-04-02	H	900
1334+039	11:32:37 2004-04-02	H	3600
1626+368	12:46:04 2004-04-02	H	3600
1633+433	14:13:36 2004-04-02	H	3600
1633+572	15:22:16 2004-04-02	H	960
1953-011	05:09:33 2004-09-30	H	3600
2140+207	06:27:51 2004-09-30	H	3600
2246+223	07:44:44 2004-09-30	H	3600
2341+321	09:56:37 2004-09-30	H	4680

Table 3. Extragalactic Objects

Name	RA	Dec	H
DSW 1	02 11 20.67	+39 55 19.2	20.5
DGF 1	10 57 34.75	-07 31 22.8	19.8
DGF 2	10 57 34.63	-07 31 13.8	20.2
DGF 3	10 57 35.15	-07 31 11.5	20.5
DGF 4	11 24 12.82	+21 21 23.9	19.7
DGF 5	21 42 40.97	+20 59 49.5	19.0
DGF 6	21 42 41.71	+20 59 46.9	20.2
DGF 7	22 49 05.83	+22 36 37.3	19.0

Table 4. Sensitivities

WD	Excess Limit (M_J)	Mass (M_{Jup})	Sensitivity $>1''$ (H)	Mass (M_{Jup})
0501+527 (1 Gyr)	15.6	75	19.8	25
(5 Gyr)		80		42
(10 Gyr)		80		63
0912+536	14.8	46	21.3	12
1055-072	15.0	46	20.9	14
1121+216	14.6	44	21.3	11
1213+528	-	-	18.0	29
1334+039	14.8	65	21.9	18
1626+368	14.2	52	21.1	14
1633+433	14.7	48	20.9	14
1633+572	14.8	54	20.5	19
1953-011	14.5	43	20.8	10
2140+207	14.1	49	21.5	10
2246+223	14.4	41	22.3	9
2341+321	13.0	69	22.4	13

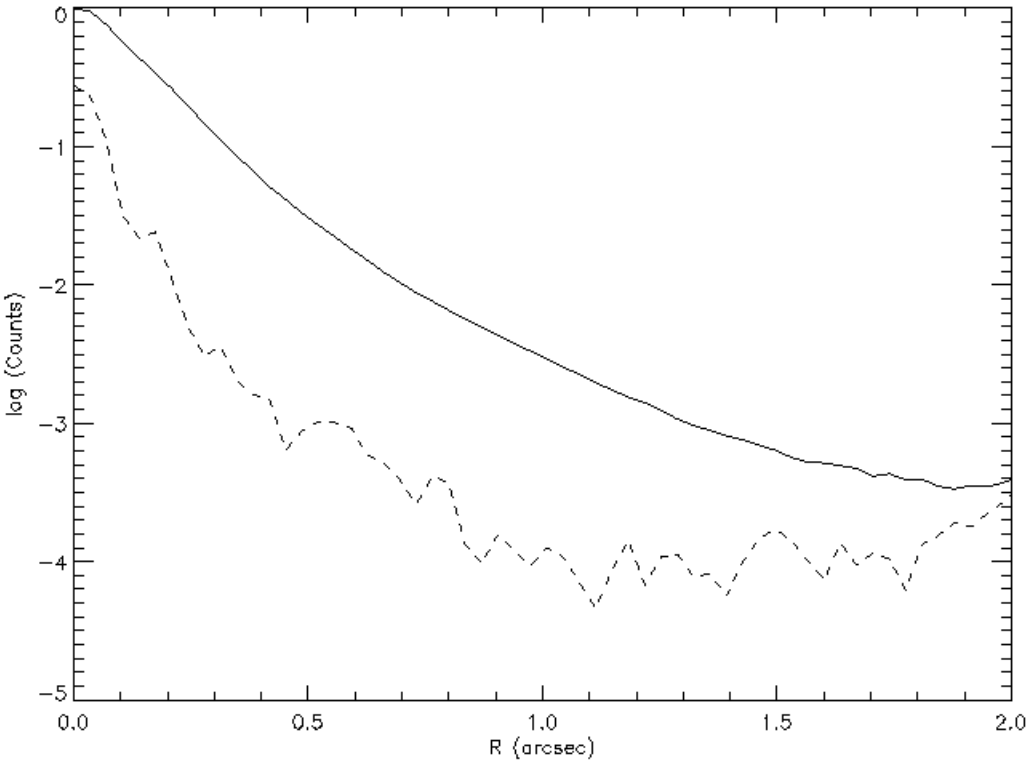

Fig. 1.— Two azimuthally averaged PSFs for WD 1953-011, before subtraction (solid line) and after subtraction (dashed line). This WD had a contemporaneous PSF reference in the field which was used for subtraction purposes.

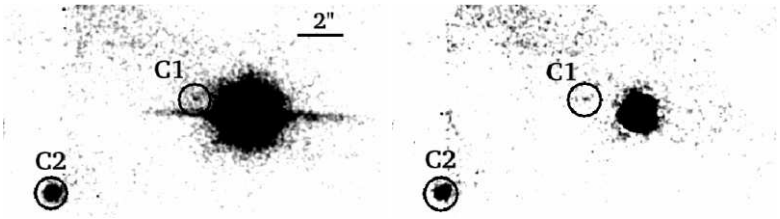

Fig. 2.— Candidate companion (C1) at a separation of 2.25″. If this object is physically associated it would be an $11 M_{Jup}$ object.

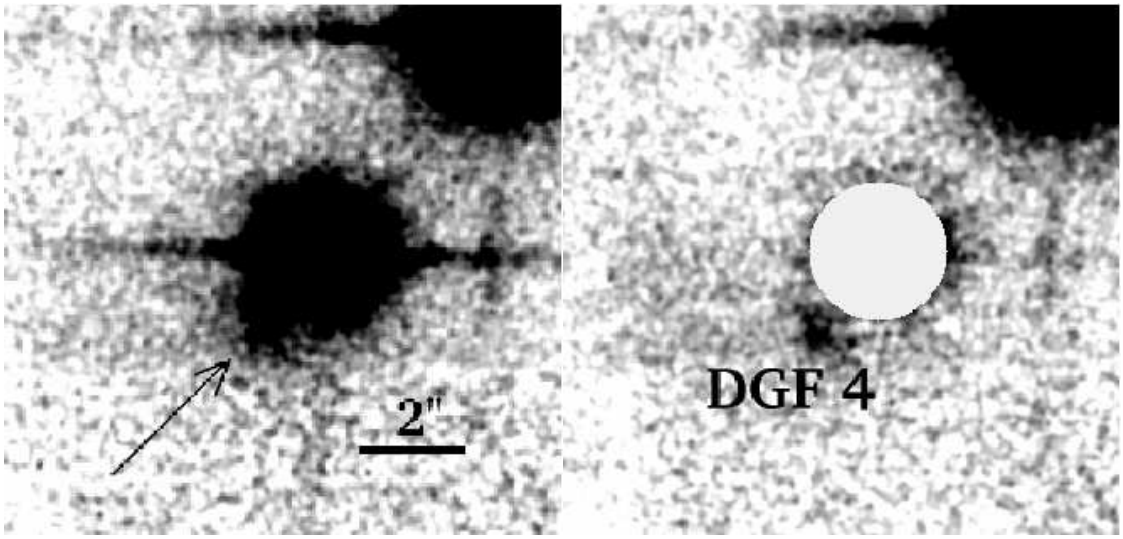

Fig. 3.— These images show extended emission discovered around WD 1121+216 before (left panel) and after (right panel) PSF subtraction. Second epoch POSS images show that it is a background galaxy. The scale bar in the left panel represents 2″.

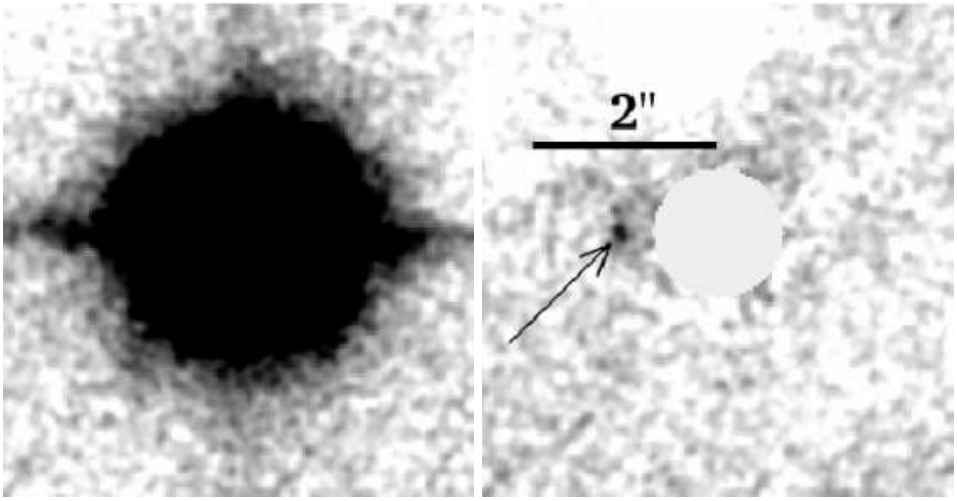

Fig. 4.— Images of a nearby background star near WD 1953-011 that show a companion with ΔH=7.6 with a separation of 1.08″ before (left panel) and after (right panel) PSF subtraction. This detection demonstrates the study's sensitivity to point sources close to our targets.

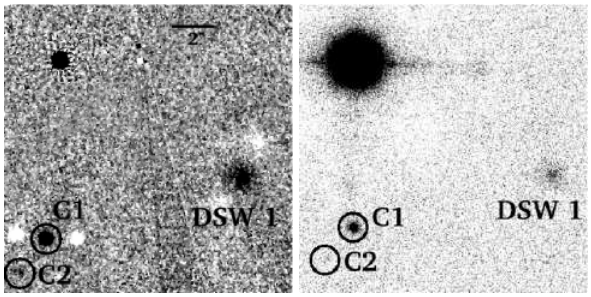

Fig. 5.— A comparison between the HST and CFHT fields for WD 0208+395. The HST field is on the left and the CFHT field is on the right. The images are about 9″ long on a side and shows one of the candidates due South of WD 0208+396 which is masked.

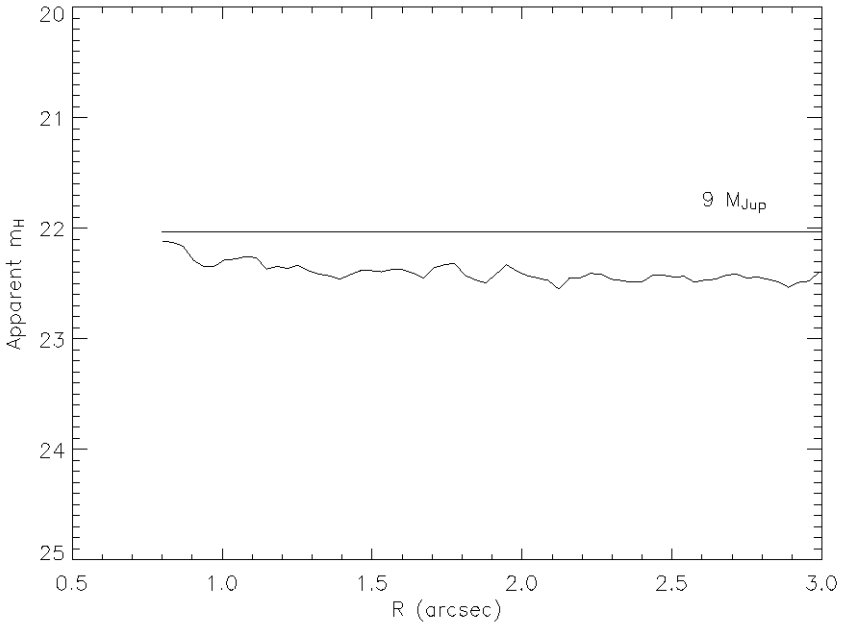

Fig. 6.— Sample 5σ sensitivity curve of WD 2246+223. Overplotted is the H magnitude of a 9 M_{Jup} companion at the age and distance of the target.

.